THE UNIVERSITY OF TENNESSEE KNOXVILLE

SME North American Manufacturing Research Conference (NAMRC 52)

AFSD-Physics: Exploring the governing equations of temperature evolution during additive friction stir deposition by a human-AI teaming approach

Tony Shi[a, b], Mason Ma[a, b] , Jiajie Wu[a, b], Chase Post[a], Elijah Charles[b], Tony Schmitz[b, c]

[a]Manufacturing Intelligence and Dynamic Systems (MINDS) Laboratory, University of Tennessee, Knoxville
[b]Machine Tool Research Center, University of Tennessee, Knoxville
[c]Oak Ridge National Laboratory

hma19@vols.utk.edu
June 21, 2024

Research objective

Demonstrate a modeling effort to explore the underlying physics of temperature evolution during additive friction stir deposition (AFSD) by a human-AI teaming approach.

Outline

- Introduction
- Human-AI teaming for AFSD temperature modeling
- Proposed AFSD-Physics
- Main results: Acquired governing equations
- Experimental setup
- Computational experiments
- Additional experimental validation
- Conclusions and outlook

Introduction

Outline

- Introduction
- Human-AI teaming for AFSD temperature modeling
- Proposed AFSD-Physics
- Main results: Acquired governing equations
- Experimental setup
- Computational experiments
- Additional experimental validation
- Conclusions and outlook

Additive friction stir deposition (AFSD)

Characteristics

- No melting: Solid state additive manufacturing process that deposits metal using plastic flow without melting
- Geometry and microstructure are produced during layer-by-layer severe plastic deformation
- Heat generation and heat transfer

Advantages

- Lower porosity
- Uniform and homogenous microstructure along the joints
- Lower residual stress
- Suitable for a wide range of materials
- High build rate
- Energy-saving

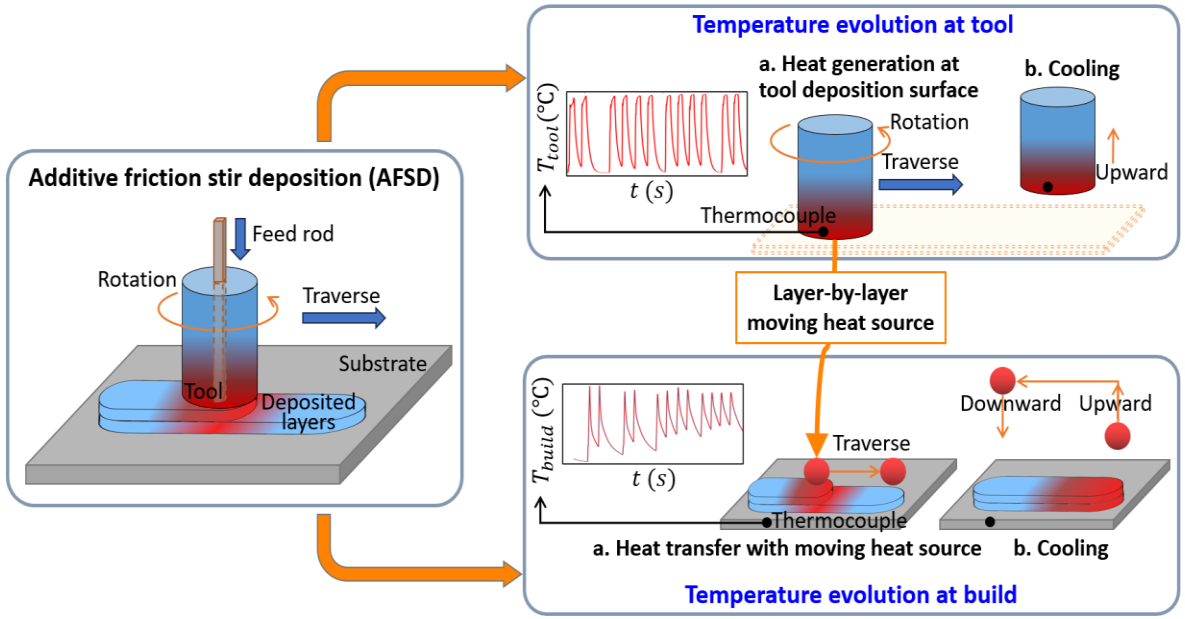

Figure from Shi et al., 2024

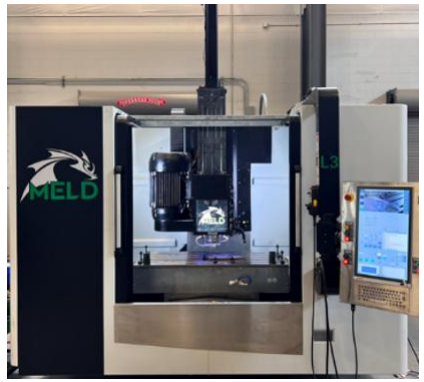

MELD MANUFACTURING

Related work for AFSD temperature modeling

- *Multiphysics process models (In nascent stage)*
  - Mesh-free based, SPH (Stubblefield et al., 2021, 2022)
  - Mesh based: FVM (Kincaid et al., 2023), FEM (Joshi et al., 2022; Sharma et al., 2022), CFD (Gotawala and Yu, 2023)
  - Limitations include: 1) limitations including boundary instability, 2) high computational cost, 3) poor scalability for multi-layer depositions, and 4) not well-suited for combination with in-process data for accuracy improvement
- *Empirical models*
  - Power law relationships with respect to spindle speed and traverse speed for predicting peak temperatures of Cu and Al-Mg-Si (Garcia et al., 2020)
- *Machine learning models*
  - AFSD-Nets for temperature evolution under the context of multi-layer deposition (Shi et al., 2024)
  - Limitations: Not physically interpretable; unstable to deal with out-of-distribution input

In-process measurements

- Controller data & external sensors data: Measurable physical variables like temperature, spindle speed, spindle torque, tool location, and actuator force applied to the feedstock for AFSD
- The unknown physics embedded in these in-process measurements has not been efficiently explored and utilized by existing ML methods.

Research gap: Experimentally verified governing equations are not available that can describe the mathematical relationship between temperature evolution at the tool-deposition and other measurable in-process physical variables

Human-AI teaming for AFSD temperature modeling

Outline

- Introduction
- Human-AI teaming for AFSD temperature modeling
- Proposed AFSD-Physics
- Main results: Acquired governing equations
- Experimental setup
- Computational experiments
- Additional experimental validation
- Conclusions and outlook

First principles for human-desired models

1. The thermodynamics phenomena dependent on operating parameters (control variables) for the tool can be formulated as nonlinear dynamic systems with control
2. Temperature evolution during layer-by-layer deposition exhibits thermal cycling as the heating and cooling steps alternate
3. Governing equations with high-accuracy and low computational cost enable real-time prediction, process control, and optimization

$$\dot{T} = f(T, \boldsymbol{u})$$

$$P^l = P^l_{heat} \cup P^l_{cool}, \qquad \forall l \in [L]$$

Human-desired models

In-process measurements

- T_{tool}: $T_{tool} = T_{tool}(t)$, tool temperature
- T_{build}: $T_{build} = T_{build}(\boldsymbol{s}, t)$, build temperature

Measurable in-process state variables by thermocouples

- ω: Tool spindle speed
- f_t: Tool feed velocity or tool traverse speed
- f_m: Feedstock feed velocity or material feed rate
- T_f: Spindle torque to overcome the friction force
- P_f: Spindle power
- T_m: Servo torque for feedstock material
- F_m: Force applied to the feedstock
- $\boldsymbol{s}_{tool}$: $\boldsymbol{s}_{tool} = (s_x, s_y, s_z)$, position of the center point
- $\boldsymbol{v}_{tool}$: $\boldsymbol{v}_{tool} = (v_x, v_y, v_z)$, velocity of the tool center

Measurable in-process state/control variables from controller

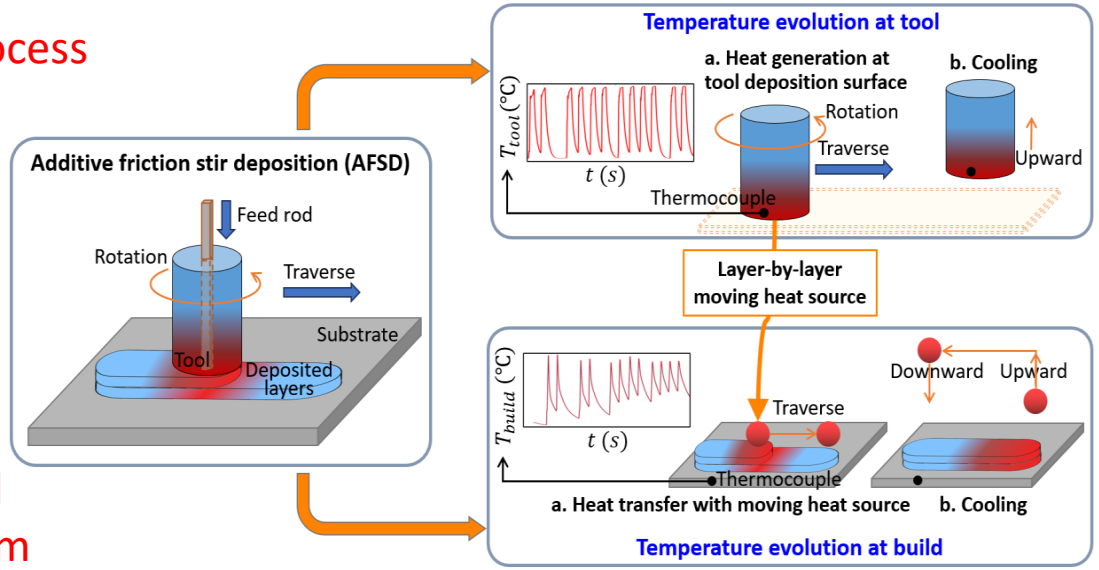

Figure from Shi et al., 2024

Fundamental research question:

How can the analytical forms of $\dot{T} = f(T, \boldsymbol{u})$ be obtained to describe the temperature evolutions at the tool and the build from in-process measurements?

- Tool temperature:

$$\dot{T}_{tool} = f(T_{tool}, \boldsymbol{u})$$

- Build temperature:

$$\dot{T}_{build} = f(T_{build}, T_{tool}, \boldsymbol{u})$$

  - where $\boldsymbol{u}$ can consist of all measurable process variables, e.g., those identified in previous slide

$$\dot{T} = f(T, \boldsymbol{u})$$

$$P^l = P^l_{heat} \cup P^l_{cool}, \qquad \forall l \in [L]$$

Human-desired models

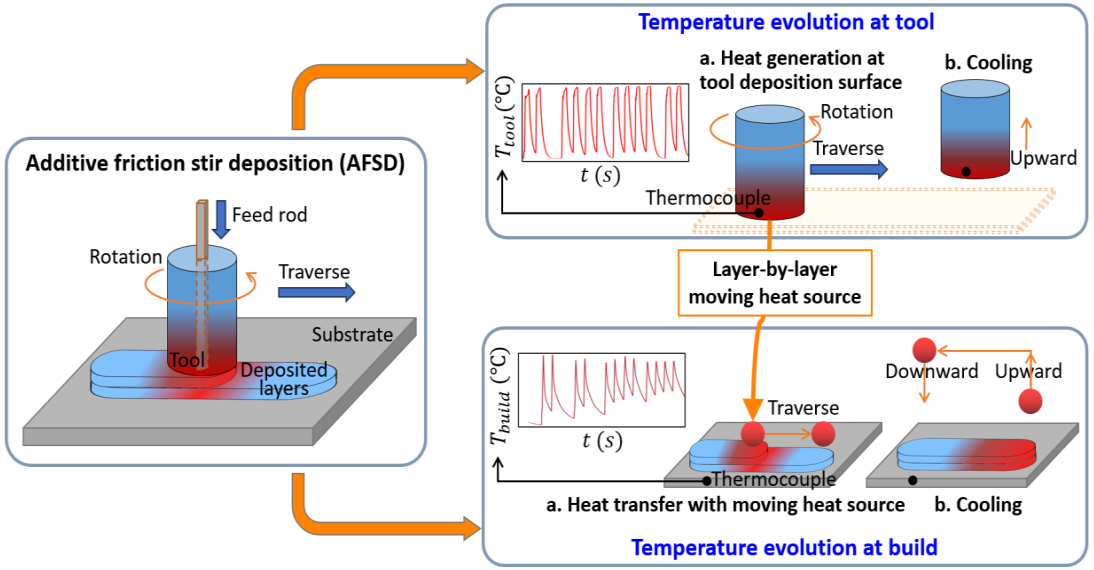

Figure from Shi et al., 2024

Idea:

Human gives initial modeling by first principles; Let **AI** help human to identify governing equations based on human initial modeling with in-process data.

Overview of the proposed human-AI teaming approach

- **Step 1**: Initial human modeling by first principles.
- **Step 2**: Design of experiments for data collection.
- **Step 3**: Human-informed machine learning modeling.
  1. Design of human-informed learning function space
  2. Design of loss function and optimization algorithm
  3. Learning process to acquire governing equations
- **Step 4**: Feedback to human for further decision making.

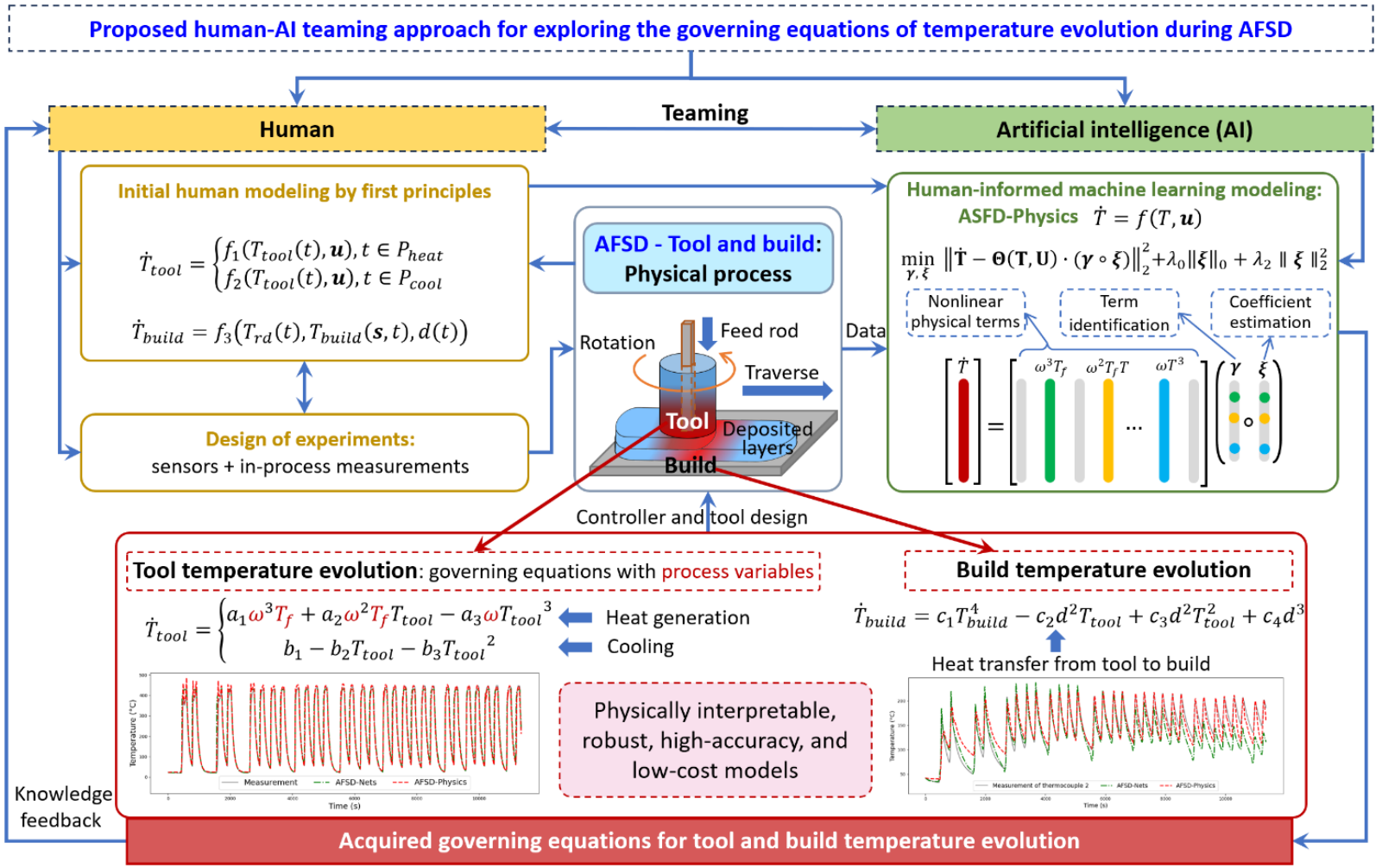

Proposed AFSD-Physics

Outline

- Introduction
- Human-AI teaming for AFSD temperature modeling
- Proposed AFSD-Physics
- Main results: Acquired governing equations
- Experimental setup
- Computational experiments
- Additional experimental validation
- Conclusions and outlook

Step 1: Initial human modeling by first principles

- *Modeling for the tool temperature*

$$\dot{T}_{tool} = \begin{cases} f_1(T_{tool}(t), \boldsymbol{u}), & t \in P_{heat}^{l}, l \in [L], \\ f_2(T_{tool}(t), \boldsymbol{u}), & t \in P_{cool}^{l}, l \in [L]. \end{cases}$$

Heat generation

Tool cooling

Assumption: the rotating deposit is a single point moving heat source and its temperature $T_{rd}(t)$ is equal to the tool temperature

$$T_{rd}(t) = T_{tool}(t)$$

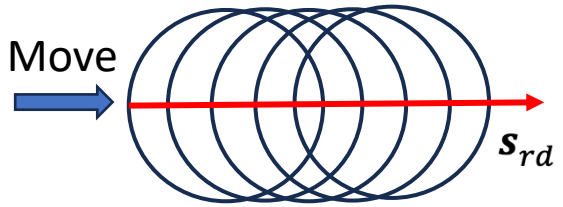

The trajectory of sensor along tool movement

- *Modeling for build temperature*

$$\dot{T}_{build} = f_3\left(T_{rd}(t), T_{build}(\boldsymbol{s}, t),\ d(t)\right),$$
$$t \in P_{heat}^{l} \cup P_{cool}^{l},\ l \in [L],$$
$$\boldsymbol{s} \in \boldsymbol{S}, \text{ and } \boldsymbol{S} = \{\boldsymbol{s}_1, \boldsymbol{s}_2, \boldsymbol{s}_3, \boldsymbol{s}_4\}$$
$$d(t) = \| \boldsymbol{s}_{rd} - \boldsymbol{s} \|_2$$

Initial conditions

$$T_{tool}(0) = T_0, T_{build}(\boldsymbol{s}_{tc}, 0) = T_0^{\boldsymbol{s}_{tc}}$$

S_{tc}: location of the thermocouple in the substrate

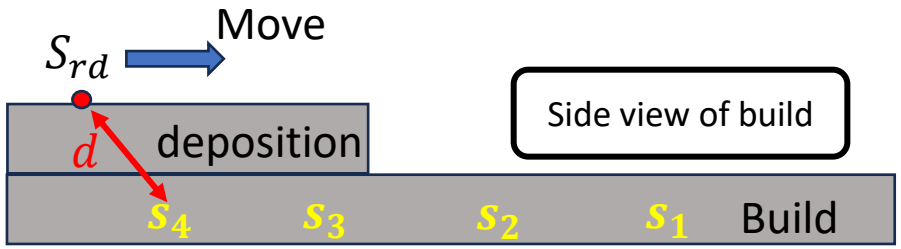

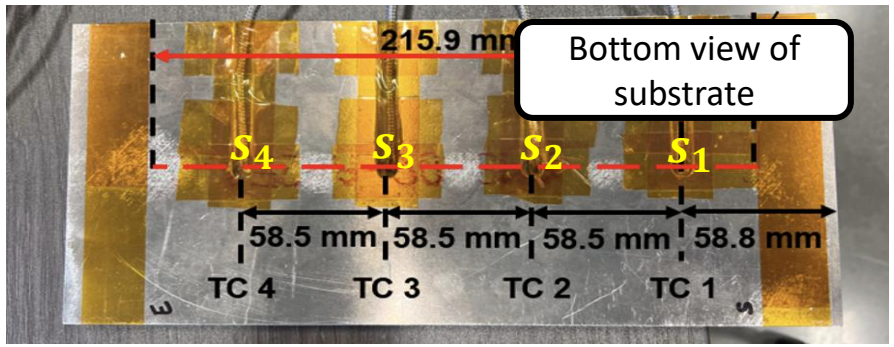

Step 2 for experiment design is introduced later

Step 3: Human-informed machine learning modeling

- Step 3.1. Design of human-informed learning function space for $f_1(\cdot)$, $f_2(\cdot)$, and $f_3(\cdot)$ that describe $\dot{T}_{\text{tool}}(t)$ and $\dot{T}_{build}(t)$

$$(T, \boldsymbol{u}) = [1 \;\; T \;\; \boldsymbol{u} \;\; (T \otimes T) \;\; (\boldsymbol{u} \otimes \boldsymbol{u}) \;\; (T \otimes \boldsymbol{u}) \;\; \cdots \;\;]$$

$$f(T, \boldsymbol{u}) = \boldsymbol{\theta}(T, \boldsymbol{u}) \cdot \boldsymbol{\xi} \Longrightarrow \text{Learning function space}$$

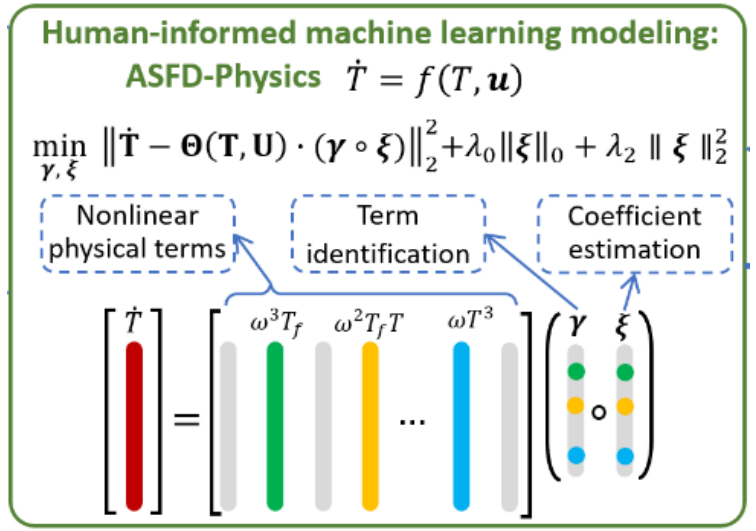

- Step 3.2. Design of loss function and optimization algorithm

$$\min_{\boldsymbol{\xi}} \left\|\dot{\mathbf{T}} - \boldsymbol{\Theta}(\mathbf{T}, \mathbf{U}) \cdot \boldsymbol{\xi}\right\|_2^2 + \lambda_0 \|\boldsymbol{\xi}\|_0 + \lambda_2 \| \boldsymbol{\xi} \|_2^2 \Longrightarrow \text{Loss function}$$

$$\langle \boldsymbol{\gamma}^*, \boldsymbol{\theta}^* \rangle = \underset{\langle \xi, \gamma \rangle \in \Delta}{\operatorname{argmin}} \left\|\dot{\mathbf{T}} - \boldsymbol{\Theta}(\mathbf{T}, \mathbf{U}) \cdot \boldsymbol{\xi}\right\|_2^2 + \lambda_2 \|\boldsymbol{\xi}\|_2^2, \text{ where } \Delta := \left\{ \langle \boldsymbol{\xi}, \boldsymbol{\gamma} \rangle \;\middle|\; \begin{matrix} -M\gamma \le \xi \le M\gamma, \; \boldsymbol{\gamma}^T e = k, \\ \xi \in \mathbb{R}^{P \times 1}, \gamma \in \mathbb{B}^{P \times 1} \end{matrix} \right\}$$

$$\gamma_p = \begin{cases} 1, & \text{if } f(\boldsymbol{u}) \text{ includes } \theta_p \\ 0, & \text{otherwise} \end{cases}, \quad \forall p \in [P].$$

$\Longrightarrow$ Discrete optimization or mixed integer optimization (MIO) algorithm

- Step 3.3. Learning process by solving MIO problem with off-the-shelf discrete optimization solvers

Main results: Acquired governing equations

Outline

- Introduction
- Human-AI teaming for AFSD temperature modeling
- Proposed AFSD-Physics
- Main results: Acquired governing equations
- Experimental setup
- Computational experiments
- Additional experimental validation
- Conclusions and outlook

- **Acquired governing equation for tool temperature evolution**

ωT_f refers to spindle power, thus $\omega^3 T_f$ and $\omega^2 T_f\ T_{tool}$ can relate to underlying heat generation mechanisms in addition to friction power

$$\dot{T}_{tool} = \begin{cases} a_1\omega^3 T_f + a_2\omega^2 T_f T_{tool} - a_3\omega {T_{tool}}^3, & t \in P_{heat} \\ b_1 - b_2 T_{tool} - b_3 {T_{tool}}^2, & t \in P_{cool}, \end{cases}$$

Newton's law of cooling

May be the additional cooling effect from the external water jacket

  - $\boldsymbol{a} = [a_1\ a_2\ a_3]$ and $\boldsymbol{b} = [b_1\ b_2\ b_3]$ are the vectors of constant coefficients

- **Acquired governing equation for build temperature evolution**

$$\dot{T}_{build} = c_1 T_{build}^4 - c_2 d^2 T_{tool} + c_3 d^2 T_{tool}^2 + c_4 d^3, \qquad t \in P_{heat} \cup P_{cool}$$

ODE with time variant parameter $d(t)$. The spatial information of the location $\boldsymbol{s} \in \boldsymbol{S}$ in the substrate is implicitly included in $d(t)$

  - $\boldsymbol{c} = [c_1\ c_2\ c_3\ c_4]$ is the vector of constant coefficients

$$\dot{T}_{tool} = \begin{cases} a_1\omega^3 T_f + a_2\omega^2 T_f T_{tool} - a_3\omega {T_{tool}}^3, & t \in P_{heat} \quad (1) \\ b_1 - b_2 T_{tool} - b_3 {T_{tool}}^2, & t \in P_{cool}, \quad (2) \end{cases}$$

$$\dot{T}_{build} = c_1 T_{build}^4 - c_2 d^2 T_{tool} + c_3 d^2 T_{tool}^2 + c_4 d^3, \qquad t \in P_{heat} \cup P_{cool} \quad (3)$$

- **How to use the acquired governing equations → time domain simulation**

Type I simulation: A new initial value is given for each layer of simulation
- The heat generation in (1) and tool cooling in (2) is simulated independently.
- The measurement at the beginning of each layer is used to set the initial value.
- **Scenario**: in-process temperature measurements are available to calibrate the simulation layer-by-layer

Type II simulation: A single initial value for the entire multi-layer simulation.
- The initial value of the next layer is set to be the last value of the previous layer.
- Coupled simulation of heat generation and tool cooling and build temperature evolution in (3).
- **Scenario**: no in-process temperature measurements are available and only the room temperature is used to start the simulation.

Experimental setup

Outline

- Introduction
- Human-AI teaming for AFSD temperature modeling
- Proposed AFSD-Physics
- Main results: Acquired governing equations
- Experimental setup
- Computational experiments
- Additional experimental validation
- Conclusions and outlook

Step 2. Design of experiments for data collection

In-process measurements recorded by controller

- Spindle speed ω
- Spindle torque T_f
- Tool traverse speed f_t
- Material feed rate f_m
- Speedle power P_f
- Servo torque for feedstock material T_m
- Force applied to feedstock F_m
- Tool center point position s_{tool}
- Tool center velocity at the bottom surface v_{tool}

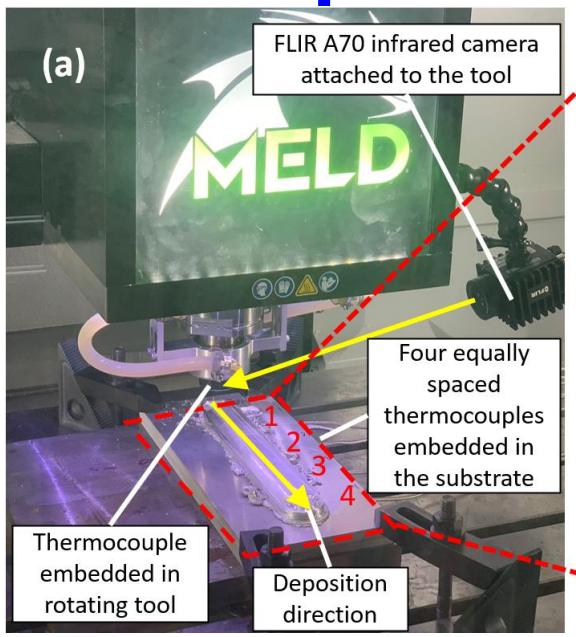

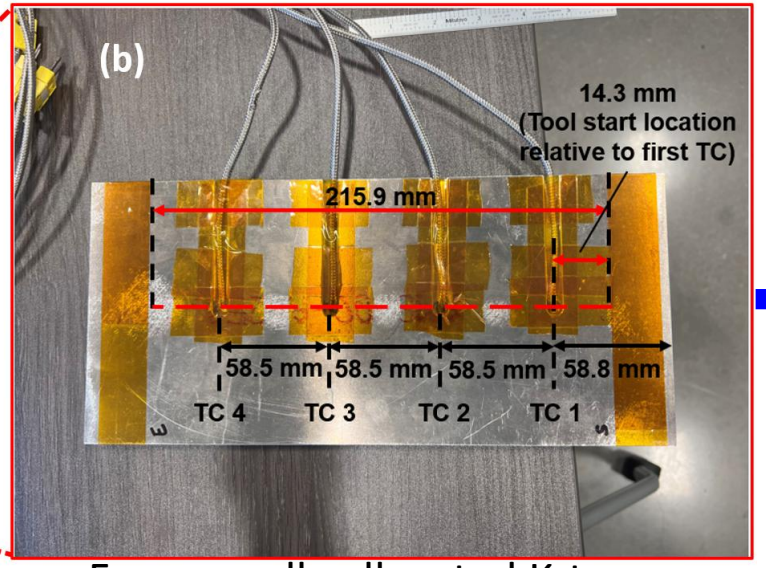

Four equally allocated K-type thermocouples (KTC) in the build

Data from external sensors: tool embedded thermocouple and four thermocouples in the build

- Tool head temperature T_{tool}
- Temperature at thermocouple T_{build}

Physical experiments

- MELD Manufacturing L3 machine
- Thermocouples are installed to collect temperature data at tool and four locations at substrate
- Deposit Aluminum 7075 feedstock 9.53 mm × 9.53 mm × 508 mm with spindle speed RPM 135
- Data is collected for the wall deposition of 30 layers
- 11358 data points for **135-rpm** dataset

Computational experiments

Outline

- Introduction
- Human-AI teaming for AFSD temperature modeling
- Proposed AFSD-Physics
- Main results: Acquired governing equations
- Experimental setup
- Computational experiments
- Additional experimental validation
- Conclusions and outlook

- **Training and testing dataset**
  - *Training data*: 5-th to 20-th layer of 135-rpm dataset
  - *Testing data*: 21-th to 30-th layer of 135-rpm dataset
  - *First 5 layers*: discarded due to poor data quality at the initial deposition
  - *Note*: only measurements from the first three thermocouples (KTC1, KTC2, KTC3) are stacked as a single dataset for training, while the last thermocouple (KTC4) is purely used for testing.
- **Parameter settings for AFSD-Physics**
  - $M = 1000$, $k \in \{3,4,5\}$, and $\lambda_2 = 100$; the best k value is selected after a preliminary tuning
  - Four order polynomials $\boldsymbol{\theta}(T, \boldsymbol{u})$ to construct function space
  - *Features for tool temperature*: heat generation – tool temperature T_{tool}, spindle speed ω, spindle torque T_f, feedstock feed speed f_m, and actuator force F_m; tool cooling – tool temperature T_{tool}
  - *Features for build temperature*: tool temperature T_{tool}, build temperature T_{build}, and the distance d
  - MIO solved by MIO solver CPLEX 20.1 with Python version
- **Comparison metrics: mean absolute percentage error (MAPE)**

$$MAPE = \frac{1}{N}\sum_{i=1}^{N}\frac{|T_i - \hat{T}_i|}{T_i} \times 100\%$$

- **All $\hat{T}_i$ is obtained by time domain simulations**

Type I simulation: A new initial value is given for each layer of simulation

Type II simulation: A single initial value for the entire multi-layer simulation

	AFSD-Nets	AFSD-Physics
Physical process decomposition / Data segmentation	Heat generation and cooling at tool; heat transfer at build	Heat generation and cooling at tool; heat transfer at build
Acquired models	Three black box NNs	Three white box ODEs
Model interpretability	Non-physically interpretable	Physically interpretable

Comparison method: AFSD-Nets from Shi et al., 2024

Type I Time-domain simulation for tool heat generation temperature evolution

- AFSD-Physics outperforms AFSD-Nets for both model accuracy and computational time on both training and testing sets
- AFSD-Physics captures the transient temperature evolution: first peak value (V-shaped valley) when the spindle speed is decreased from 350 rpm (for quick heating and softening of the feedstock) to 135 rpm (for deposition)

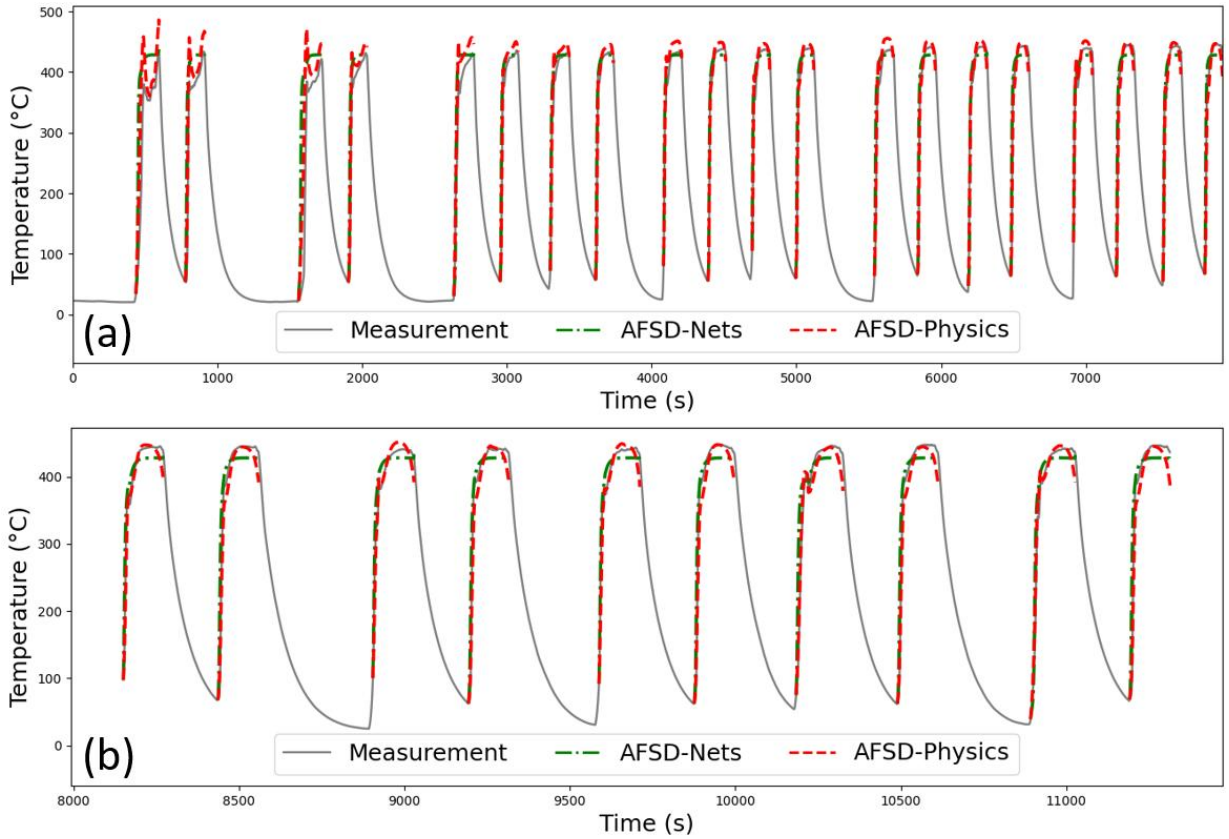

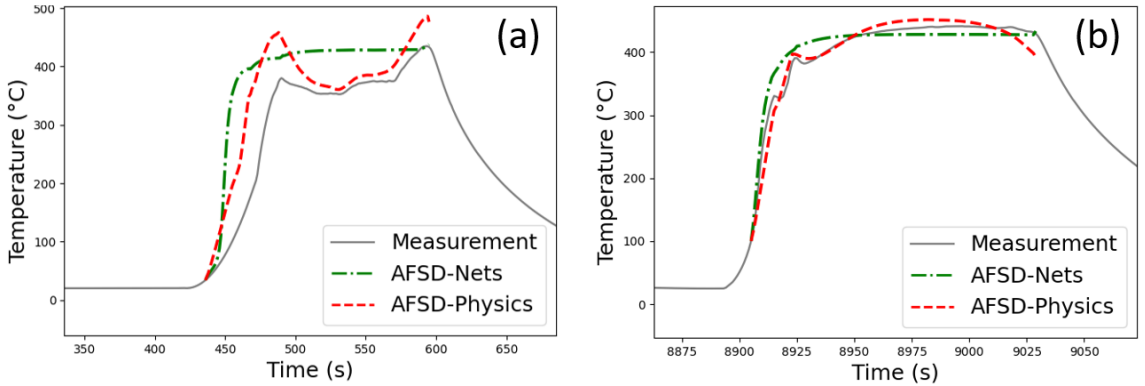

Table 2. MAPE and simulation time comparison for Type I simulation (a new initial value for each layer) of heat generation stage.

Dataset	AFSD-Nets		AFSD-Physics	
	MAPE (%)	Time (s)	MAPE (%)	Time (s)
Training set, 135-rpm	18.5429	0.6882	**10.2894**	**0.1566**
Testing set, 135-rpm	7.3858	0.4169	**3.7789**	**0.1496**

Type I Time-domain simulation for tool cooling temperature evolution

- AFSD-Physics outperform AFSD-Nets on testing set for both model accuracy and computational time
- AFSD-Nets overfits on the training set with better model accuracy

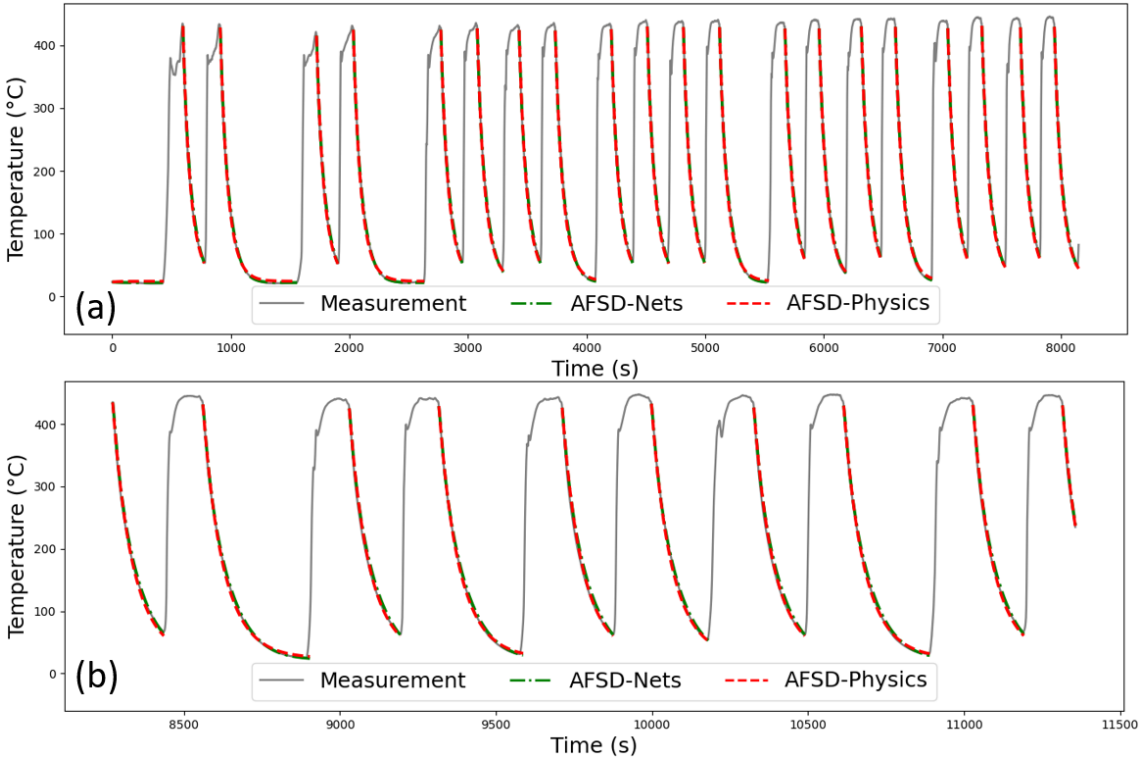

Table 3. MAPE and simulation time comparison for Type I simulation (a new initial value for each layer) of tool cooling stage.

Dataset	AFSD-Nets		AFSD-Physics	
	MAPE (%)	Time (s)	MAPE (%)	Time (s)
Training set, 135-rpm	**2.9297**	5.1711	5.8811	**3.3623**
Testing set, 135-rpm	3.825	3.5413	**3.525**	**3.3489**

Type II Time-domain simulation for tool head temperature evolution – coupled heat generation and tool cooling

- AFSD-Physics outperforms AFSD-Nets on both model accuracy and computational time
- AFSD-Physics effectively captures the valley-shaped heat generation pattern between two peak temperature values
- Generalization capability of AFSD-Physics:
  - Only the data from 5th to 20th layer are used for training
  - Single initial point at layer 1 is used for simulation

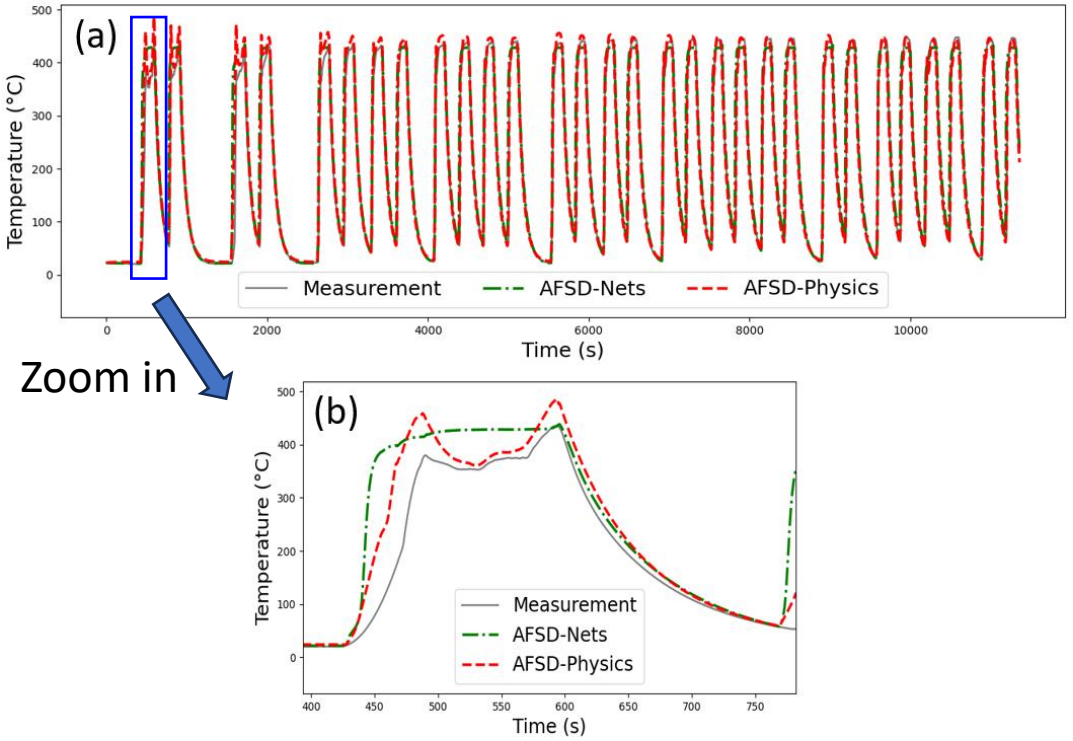

Table 4. MAPE and simulation time comparison for Type II simulation (a single initial value for the entire multi-layer simulation) of tool temperature.

Dataset	AFSD-Nets		AFSD-Physics	
	MAPE (%)	Time (s)	MAPE (%)	Time (s)
135-rpm dataset	14.5670	5.7751	**9.3273**	**4.2441**

Type II Time-domain simulation for build temperature evolution – heat transfer

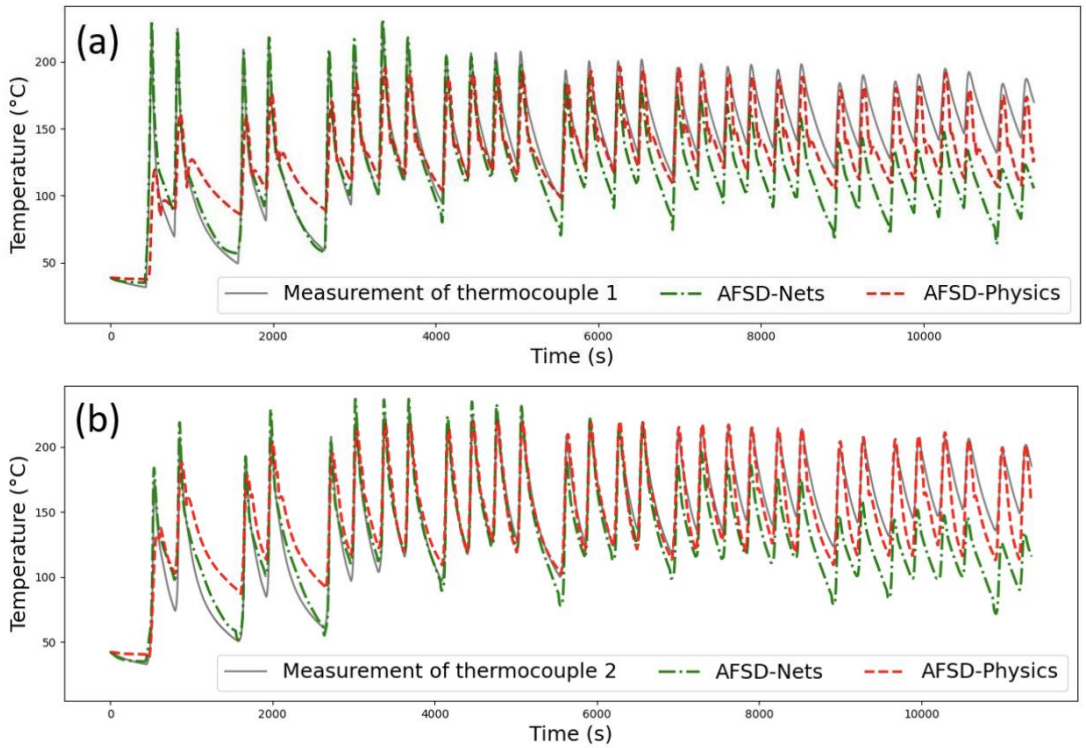

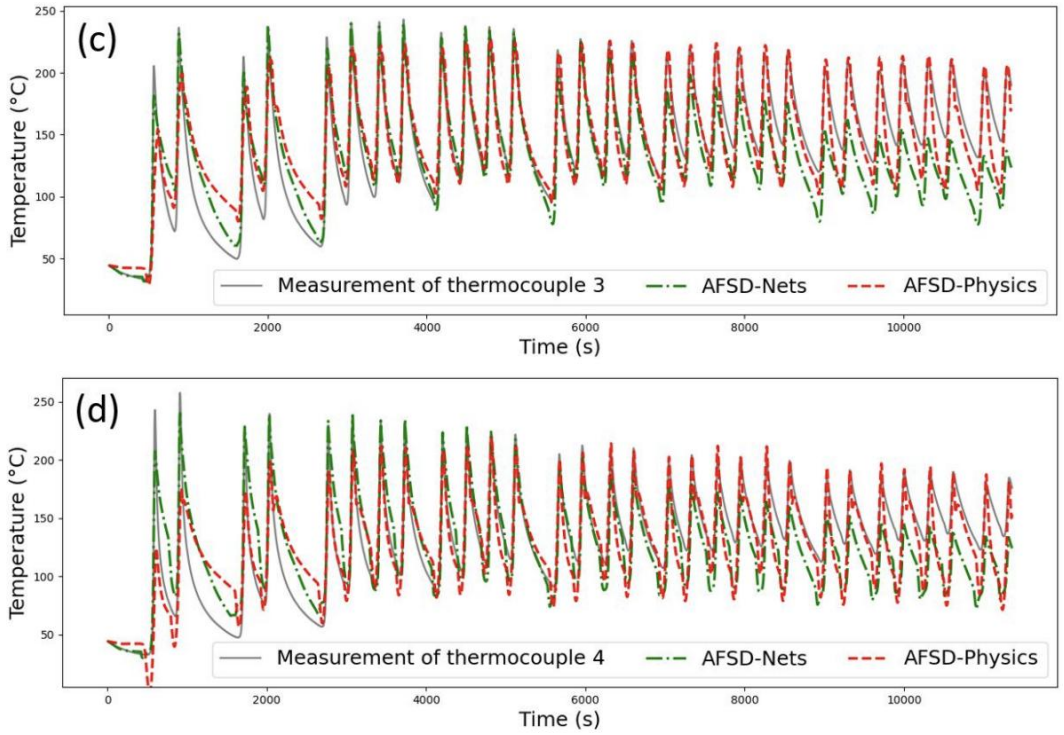

Table 5. MAPE and simulation time comparison for Type II simulation (a single initial value for the entire multi-layer simulation) of build temperature.

Thermocouple	AFSD-Nets		AFSD-Physics	
	MAPE (%)	Time (s)	MAPE (%)	Time (s)
KTC1	17.0176	2.3051	**14.2840**	**0.1177**
KTC2	14.7449	2.3011	**12.9856**	**0.1057**
KTC3	15.7802	2.4982	**14.1893**	**0.1087**
KTC4	19.8777	2.1001	**17.6206**	**0.1044**

- AFSD-Physics outperforms AFSD-Nets for model accuracy and computational time
- In general, AFSD-Physics is better at capturing overall trend and peak values, but with more deviation at the intersection of two different physical stages than AFSD-Nets
- Generalization capability: KTC4 in (d) is completely extrapolation

Type II Time-domain simulation for build temperature evolution – heat transfer

- 1D prediction of temperature on the centerline
- It also shows the potential for 2D/3D temperature maps by integrating more spatial in-process measurements

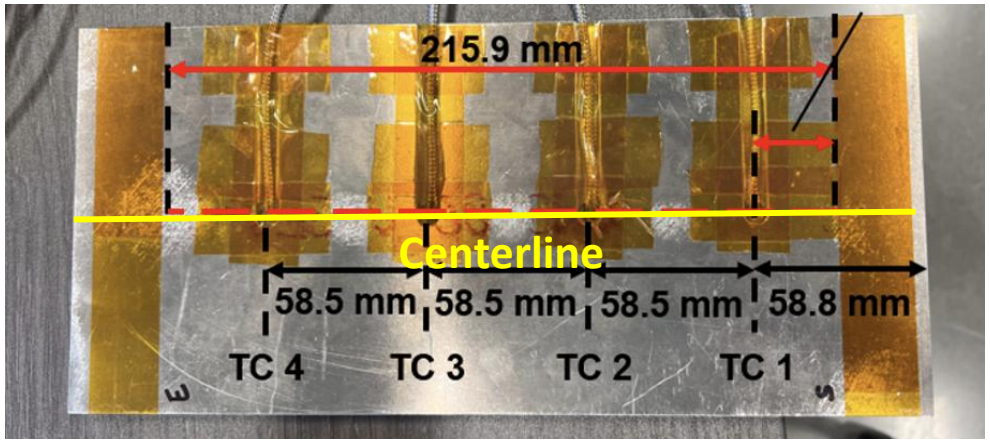

The substrate

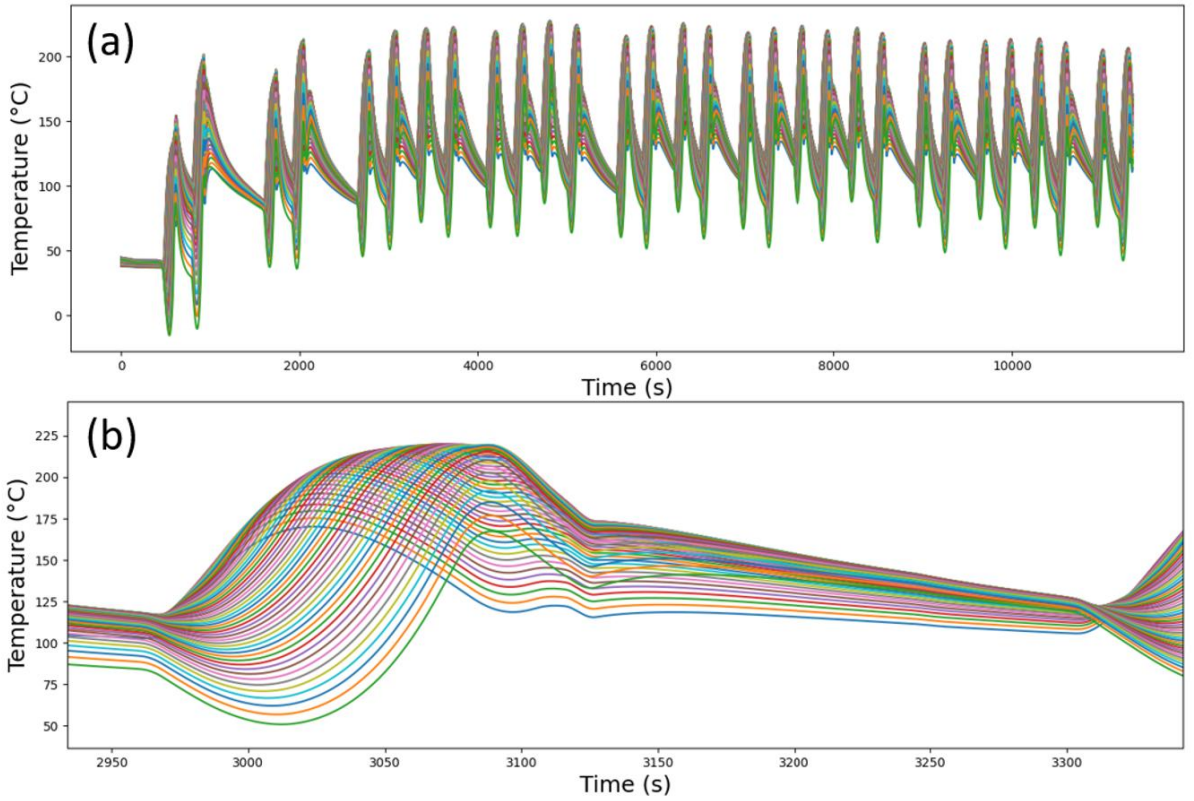

Figure 8. (a) Simulation results of the build temperature for 53 interpolation locations on the centreline of substrate where four thermocouples are located. (b) Zoom-in plots of one-layer build temperature simulation.

Additional experimental validation

Outline

- Introduction
- Human-AI teaming for AFSD temperature modeling
- Proposed AFSD-Physics
- Main results: Acquired governing equations
- Experimental setup
- Computational experiments
- Additional experimental validation
- Conclusions and outlook

Step 4: Robustness and generalizability for tool temperature as a demonstration of feedback mechanism

Idea: Use the same experimental setting as 135 RPM except for a new spindle speed 115 RPM adopted for deposition

- 7782 data points after data preprocessing, denoted by 115-rpm dataset

- The same set of governing equations are stably acquired for data from 115-rpm, and combined 135&115 datasets

$$\dot{T}_{tool} = \begin{cases} a_1\omega^3 T_f + a_2\omega^2 T_f T_{tool} - a_3\omega {T_{tool}}^3, t \in P_{heat}, \\ b_1 - b_2 T_{tool} - b_3 {T_{tool}}^2, \quad t \in P_{cool}. \end{cases}$$

- Same physical terms: acquired governing equations capture the main physical mechanisms for tool-deposition temperature evolution

- Different coefficients: these parameters are process dependent

Table 6. Parameter values of the acquired governing equations using dataset 135-rpm, 115-rpm, and their combination.

Parameter	AFSD-Physics: 135	AFSD-Physics: 115	AFSD-Physics: 135&115
a_1	2.7640×10^{-9}	2.1621×10^{-9}	2.8781×10^{-9}
a_2	1.8361×10^{-9}	1.7824×10^{-9}	1.6599×10^{-9}
a_3	1.1382×10^{-8}	1.1865×10^{-8}	1.0621×10^{-8}
b_1	0.3283	0.0198	0.1187
b_2	0.0135	0.0044	0.0083
b_3	6.06×10^{-6}	2.7474×10^{-5}	1.8550×10^{-5}

Step 4: Robustness and generalizability for tool temperature as a demonstration of feedback mechanism

- Model using 135&115-rpm dataset performs in between the model using only 135-rpm and 115-rpm
  - Models from only 135-rpm and 115-rpm overfit to their datasets

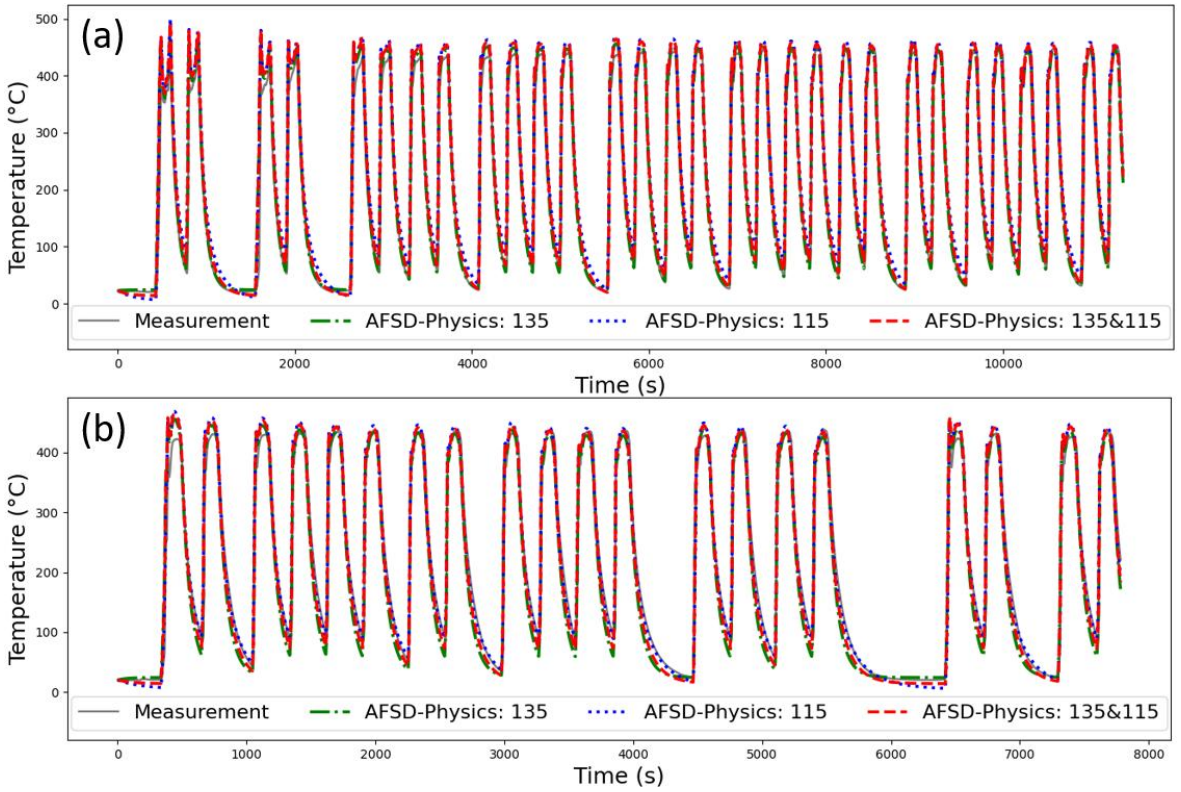

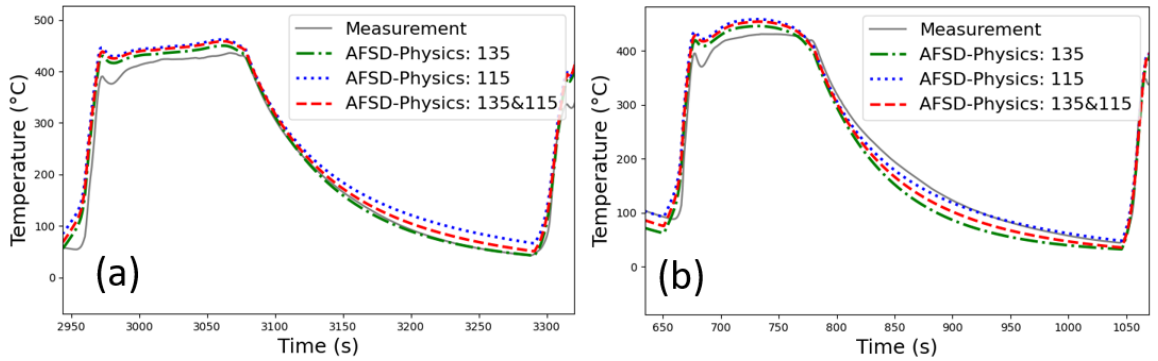

Dataset	AFSD-Physics: 135	AFSD-Physics: 115	AFSD-Physics: 135&115
135-rpm	**9.3273**	23.4318	12.7625
115-rpm	16.5819	**11.0977**	14.2969

Conclusions

Outline

- Introduction
- Human-AI teaming for AFSD temperature modeling
- Proposed AFSD-Physics
- Main results: Acquired governing equations
- Experimental setup
- Computational experiments
- Additional experimental validation
- Conclusions and outlook

- **Conclusions**:
  - **Human-AI teaming approach**: A modeling effort to explore the underlying physics of temperature evolution AFSD; a pathway to provide AI with first principles models to advance knowledge in manufacturing.
  - **AFSD-Physics**: A human-informed ML method to effectively explore the unknown physics of AFSD and learn the governing equations of temperature evolution from in-process measurements.
  - **Acquired governing equations (ODE):** provide physically interpretable, robust models with low computational cost and high accuracy. The acquired models demonstrate good generalizability and potential for applications to process parameter selection and in-process temperature controller design to improve part quality from the AFSD process

- **Future work:**
  - **Governing equations with arbitrary process parameters including tool spindle speed, feedstock feed velocity, and tool traverse speed**: Integrate analytical models with a series of representative experiments to enable the proposed human-AI teaming approach
  - Integrate **material flow constitutive models like Johnson-Cook** and the other microstructure features into the human-informed learning function space to improve temperature model capabilities for different materials.
  - Design efficient **physical model-based controllers** to achieve in-process feedback control for AFSD to produce high-performance metal parts.